

Theory of High T_c Ferromagnetism in SrB_6 family: A case of Doped Spin-1 Mott insulator in a Valence Bond Solid Phase

G. Baskaran
Institute of Mathematical Sciences
C.I.T. Campus, Madras 600 113, India

Doped divalent hexaborides such as $Sr_{1-x}La_xB_6$ exhibit high T_c ferromagnetism. We isolate a degenerate pair of $2p$ -orbitals of boron with two valence electrons, invoke electron correlation and Hund coupling, to suggest that the undoped state is better viewed as a spin-1 Mott insulator; it is predicted to be a type of 3d Haldane gap phase with a spin gap ~ 0.1 eV, much smaller than the charge gap of > 1.0 eV seen in ARPES. The experimentally seen high T_c ‘ferromagnetism’ is argued to be a complex magnetic order in disguise - either a canted 6-sublattice AFM ($\approx 120^\circ$) order or its quantum melted version, a chiral spin liquid state, arising from a type of double exchange mechanism.

The observation [1] of high T_c ‘ferromagnetism’ in lightly doped SrB_6 family is a great surprise in condensed matter physics in recent times; neither Sr nor B are known to participate in magnetism. Another surprise that followed was a high T_c superconductivity in MgB_2 , a diboride. Electron deficient B is known to form molecules and solids with varying ligancy, from the stable doubly charged octahedral $(B_6H_6)^{2-}$ molecule to a metallic phase of boron, that has B_{12} icosahedral cluster as a basic building block. How a $2p$ atom like boron in solid state manages to achieve high T_c superconductivity as well as high T_c ferromagnetism is a fascinating question.

There is sustained effort to understand ferromagnetism in the SrB_6 family. Some of the new experimental results [2–7] are intriguing and can not be explained in a satisfactory fashion by the existing theories [8–14] including the popular excitonic instability [9–13] scenario. Notable among them are the recent ARPES and x-ray emission studies [7], that show a gap > 1 eV at the Fermi level for pure SrB_6 . A gap of ~ 0.8 eV is also predicted by an electronic structure calculation [18] using GW method that attempts to incorporate correlation effects in earlier approaches [15–17].

In the present letter we propose that it is advantageous and perhaps also correct to view the SrB_6 family as a spin-1 Mott insulator, in view of strong coulomb repulsions and Hund coupling among two electrons in two degenerate valence orbitals of boron. However, at the outset we should point out that the difference between a band and Mott insulator, in an *even electron number* (per unit cell) insulator (with no magnetic order) like ours, is *quantitative* in the sense it is largely determined by whether $E_T \ll E_c$ or not. Here E_T is the spin gap or the lowest magnetic triplet exciton energy and E_c is the charge gap (as seen by ARPES for example).

Our present proposal is consistent with all the known experimental results and further certain novel predictions, which can be experimentally tested, follow in a natural fashion. i) SrB_6 is a spin-1 Mott insulator, with two

electrons in a doubly degenerate $2p$ -orbitals providing a spin-1 moment. ii) Antiferromagnetic coupling among the localized spin-1 moments, arising from kinetic exchange leads to a type of *3d Haldane gap or Majumdar-Ghosh phase with unbroken lattice symmetry* (figure 1). The singlet valence bonds are ‘frozen’ at the $B-B$ bond bridging two neighboring B_6 octahedra. This phase has a small spin gap $E_T \sim 0.1$ eV (this is not incompatible with a diamagnetic behavior of the insulating SrB_6). iii) Doping liberates, through a form of double exchange mechanism, a canted 6-sublattice AFM ($\approx 120^\circ$) order or a chiral spin liquid state, $\langle \mathbf{S}_{i\alpha} \cdot (\mathbf{S}_{i\beta} \times \mathbf{S}_{i\gamma}) \rangle \neq 0$ both with a small ferromagnetic moment. Our predictions could be tested by neutron scattering or other low energy probes. Two of our robust predictions are a small spin gap, $E_T \sim 0.1$ eV and at the least a well developed 120° spin correlations (figure 1) inside a B_6 octahedron.

The following two experimental facts about SrB_6 , when taken together are striking and gives an important clue for our model building. i) As revealed by recent ARPES experiments [7] the parent insulator has a charge gap > 1 eV ii) The insulating paramagnetic ground state is very fragile (unlike a band insulator) and a small doping in $Sr_{0.995}La_{0.005}B_6$, that adds half a percent of carrier per La atom, produces a ferromagnetic phase (with a small moment $\approx 0.07\mu_B$ per La atom) with a large $T_c \approx 600 - 900K$.

Some key quantum chemical information about the SrB_6 family that we will use in building our theory are: i) each B atom has two valence electrons and two degenerate valence p -orbitals, ii) the intra atomic Hund coupling is ≈ 1.5 eV, iii) the unscreened Hubbard U for the $2p$ orbitals of B can be as large as $8 - 10$ eV. iv) The nearest neighbor inter octahedral $B-B$ distance is smaller than that inside an octahedron by about 5 percent.

We first briefly present the conventional electronic structure [15] description of B_6 cluster in SrB_6 . B_6 octahedra are covalently bonded to form a simple cubic lattice. There is nearly complete charge transfer from Sr to B_6 cluster: $Sr^{2+}B_6^{2-}$. Ignoring the core orbitals of

B as well as Sr^{2+} we are left with one 2s and three 2p orbitals per B atom. There are 20 electrons in these 24 B orbitals in every octahedron. The 24 orbitals can be separated into two sets: i) sp^1 hybrids (two per B atom) that are along the body diagonal of the B_6 octahedra and ii) two p -orbitals per B atom that are tangential to the octahedra (inset in figure 1). An s-like combination of the six sp^1 hybrids that are pointing at the octahedral center form a very strong six center bond with a binding energy of about 15 eV. This bonding state takes two electrons and is primarily responsible for the stabilization of the octahedra. The sp^1 orbital pointing radially outwards strongly hybridize with the corresponding orbital of neighboring octahedra and results in a stable covalently bonded cubic network of B_6 octahedra. These bonding states take away 6 electrons per B_6 octahedra. *We are now left with 12 electrons and 12 p -orbitals per octahedron, i.e., two tangential 2p orbitals and two electrons per B atom.*

In the first band structure calculation [15] for SrB_6 family, Longuet-Higgins and Roberts, using the 12 p -orbitals, form a set of four triply degenerate molecular orbitals - t_{1u}, t_{2g}, t_{1g} and t_{2g} . (For simplicity we will ignore the hybridization of t_{1u} with symmetry adapted sp^1 orbitals that leads to t'_{1u} and t''_{1u}). These B_6 cluster orbitals overlap to produce 6 bonding and 6 anti bonding Bloch bands. The 6 bonding bands are completely filled by 12 electrons to produce a band insulator. Later workers [16,17] emphasized the mixing of anion d-states and showed that within band theory it reduces the band gap to nearly zero value at the X-points in k-space.

In the absence of any electron-electron interaction the energy difference between the top most t_{1g} and bottom most t_{1u} molecular orbitals is ~ 10 eV. This is a measure of the kinetic energy of delocalization per electron in the Slater determinant state within a B_6 cluster. This energy is comparable to the Hubbard $U \sim 8 - 10$ eV. In addition we have a ferromagnetic Hund coupling between two p -orbitals of a B atom, $J_H \sim 1.5$ eV. As the kinetic energy of delocalization within the cluster is comparable to the energy increase from Hubbard U and Hund coupling J_H , the low lying cluster eigen states are strongly perturbed by many body effects, to the extent the simple B_6 molecular orbitals and their Slater determinant states mostly lose their relevance.

Thus a natural starting point to understand the low energy physics of the cluster is the Mott localization of two electrons and form a spin-1 boron moment. Our approach is similar to restricting oneself to the valence band basis in the case of carbon $p\pi$ bonded system such as benzene (with very similar quantum chemical parameters), where it is known to work very well; ours is a generalization of valence bond basis approach to the case of two p -orbitals per site. Further the inter B_6 cluster hopping does not modify this localized picture significantly, as the inter molecular orbital hopping matrix element between

neighboring clusters is small ~ 0.25 eV (that leads to a band width of $12 \times 0.25 \approx 3$ eV, as seen in band structure results).

We have formalized the above by starting from a doubly degenerate 3 dimensional Hubbard model containing an average of one electron per orbital:

$$H = - \sum_{\langle ij; \alpha\beta; \mu\nu \rangle} t_{ij}^{\alpha\beta; \mu\nu} C_{i\alpha\mu\sigma}^\dagger C_{j\beta\nu\sigma} + U \sum_{i\alpha\mu} n_{i\alpha\mu\uparrow} n_{i\alpha\mu\downarrow} - J_H \sum_{i\alpha} \mathbf{s}_{i\alpha 1} \cdot \mathbf{s}_{i\alpha 2} \quad (1)$$

Here $t_{ij}^{\alpha\beta; \mu\nu}$ represents the nearest neighbor hopping integrals; i denotes the centers of octahedra that form a simple cubic lattice, $\alpha = 1, \dots, 6$ denotes a B site within an octahedron and $\mu = 1, 2$ denotes the two degenerate p -orbitals. The operator $\mathbf{s}_{i\alpha\mu}$ is a spin half operator of an electron in the μ th p -orbital of α 'th B site in the i -th octahedron.

Our Hubbard model contains three types of nearest neighbor hopping matrix elements $t_{\pi 1}$, $t_{\pi 2}$, and $t_{\pi\sigma}$ shown in the inset in figure 1; their values range over 1 eV to 1.5 eV. As mentioned earlier $U \sim 8$ eV and $J_H \sim 1.5$ eV.

To understand the low energy spin dynamics we perform a kinetic exchange perturbation theory and get a 3 dimensional spin-1 Hamiltonian for our Mott insulator:

$$H_s = J_1 \sum_{i, \langle \alpha\beta \rangle} \mathbf{S}_{i,\alpha} \cdot \mathbf{S}_{i,\beta} + J_2 \sum_{\langle ij; \alpha\beta \rangle} \mathbf{S}_{i,\alpha} \cdot \mathbf{S}_{j,\beta} \quad (2)$$

The first term represents the B_6 cluster spin Hamiltonian and second the octahedral bridge spin coupling. Here $\mathbf{S}_{i\alpha}$ is the spin-1 operator of the α 'th B atom in the i -th B_6 octahedron. J_1 and J_2 are intra cluster and inter cluster kinetic exchange integrals. A direct kinetic exchange perturbation theory gives a large antiferromagnetic coupling and it needs to be corrected by subtracting a direct or 'potential exchange' (arising from non-orthogonality of the nearest neighbor orbitals) that favors ferromagnetic alignment. We have estimated the potential exchange by looking at some experimental results and quantum chemical calculations for the related carbon systems. After making this subtraction we estimate $J_1, J_2 \sim 0.1$ to 0.3 eV and $J_1 < J_2$. In view of the approximate nature of our estimates, we will keep J_1 and J_2 as parameters to be determined experimentally.

Now we derive the phase diagram for our spin Hamiltonian as a function of its only parameter, the dimensionless ratio $\frac{J_2}{J_1}$ (figure 2). It is convenient to rewrite the Hamiltonian (equation 2) as

$$H_s = \frac{J_1}{4} \sum_{i, \langle \alpha\beta\gamma \rangle} (\mathbf{S}_{i,\alpha} + \mathbf{S}_{i,\beta} + \mathbf{S}_{i,\gamma})^2 + \frac{J_2}{2} \sum_{\langle ij; \alpha\beta \rangle} (\mathbf{S}_{i,\alpha} + \mathbf{S}_{j,\beta})^2 - N(12J_1 + 6J_2), \quad (3)$$

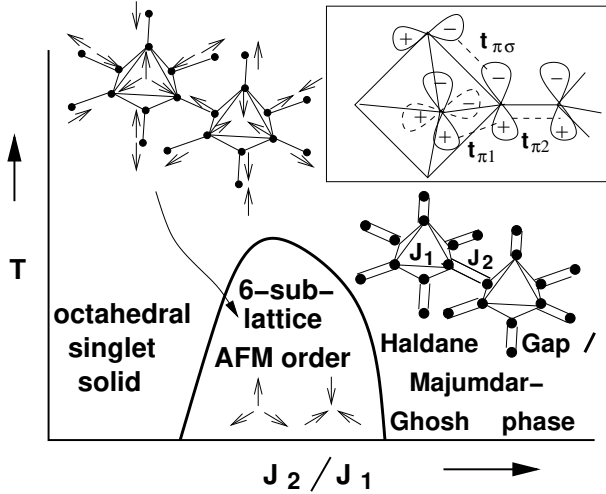


FIG. 1. Schematic phase diagram of our Boron spin-1 Hamiltonian. Doubles lines denote ‘frozen’ valence bonds at the octahedral bridges. Inset shows the ‘tangential’ boron $2p$ valence orbitals and 3 types of hopping matrix elements.

where N is the total number of octahedra. The first term of equation (3) represents the sum over triangles of three spins forming the eight faces of a B_6 octahedron. Each term of equation 3 is a positive operator with eigen values ≥ 0 . It follows immediately that the classical ground state of the above Hamiltonian is a 120° six-sublattice antiferromagnet for any $J_1, J_2 > 0$. The spin pattern within an octahedron is shown in figure 2. Spins pairs at opposite corners of an octahedron are parallel. Three such diagonal pairs within an octahedron are coplanar and at an angle of 120° , among themselves. This defines a spin chirality (vorticity) ± 1 for an octahedron. The cubic lattice of octahedra form two cubic sublattices with corresponding spins exactly anti-parallel, making it a 6-sublattice planar antiferromagnet (figure 1). The net result is that the bridge spin coupling is not frustrated, but the twelve nearest neighbor coupling within an octahedron are frustrated. In spite of the spin reversals the chirality has the same sign in all the octahedra; i.e., we have a ferromagnetic chiral order. Thus our ground state exhibits a discrete two fold chirality (Ising like) degeneracy in addition to the global $SU(2)$ spin rotational degeneracy.

For $\frac{J_2}{J_1} \approx 1$ the classical ground state exhibited above is stable and survives spin wave fluctuations. However, when $\frac{J_2}{J_1} \gg 1$ or $\frac{J_2}{J_1} \ll 1$ quantum fluctuations destabilize the classical ground state and we get singlet ground states with a finite spin gap.

When $\frac{J_2}{J_1} \ll 1$ each B_6 cluster has a unique singlet ground state. There is a finite gap $\sim J_1$ for spin-1 excitation. The couplings J_2 between neighboring octahedra through the bridge spins reduce this gap by virtual excitations. We have estimated by perturbation theory that the gap survives until $\frac{J_2}{J_1} \sim \frac{1}{2}$. We call this phase as the octahedral singlet solid (OSS).

When $\frac{J_2}{J_1} \gg 1$ the AFM order is destabilized; the octahedral bridge pairs become non-degenerate singlets with a gap of $\sim J_2$ for spin-1 excitations. Spin couplings within B_6 cluster reduce this gap by virtual excitations and the gap vanishes when we decrease $\frac{J_2}{J_1}$ to a value ~ 2 . This *valence bond solid* phase is a 3 dimensional realization of spin-1 Majumdar-Ghosh phase, that also retains the lattice symmetry. Further, this phase is also continuously connected to an AKLT [19] type of 3d Haldane gap phase, with quantum fluctuating effective spin-3 moments at B_6 clusters [20]

Where is SrB_6 family in the above phase diagram? It is unlikely that undoped SrB_6 family has long range AFM order. The shortness of the octahedral bridge $B-B$ distance by about 5 percent, compared to nearest neighbor $B-B$ distance within an octahedra seen in all the three hexaborides, SrB_6 , CaB_6 , BaB_6 could also arise, apart from some quantum chemical reasons, from the formation of a ‘frozen’ singlet (valence bond) between the B spin-1 moments of the octahedral bridge pair. So it is very likely that the strong quantum fluctuations of the spin-1 system and the fact that $\frac{J_2}{J_1} \geq 1$ in the SrB_6 family is keeping it in a valence bond solid phase.

Now we discuss how very small doping leads to a ferromagnetic order with a large curie temperature. The analysis of the doped situation starting from the Hubbard model (equation 3) is hard compared to the undoped case. However, our preliminary analysis indicates very rich possibilities, all arising from the Mott insulator parentage and the ‘vicinity’ to an antiferromagnetic order.

We believe that the observed small moment gives us an important clue as to the origin of magnetism. A natural way in which a small moment can arise is by canting of an existing antiferromagnetic order. Our valence bond solid phase, being close to the 6-sublattice AFM phase in the phase diagram, should have short range antiferromagnetic correlations. Further if doped carrier delocalization decreases the effective $\frac{J_2}{J_1}$ of our boron spin Hamiltonian, we may be pushed into the 6-sublattice AFM phase: we argue below that this is likely to happen.

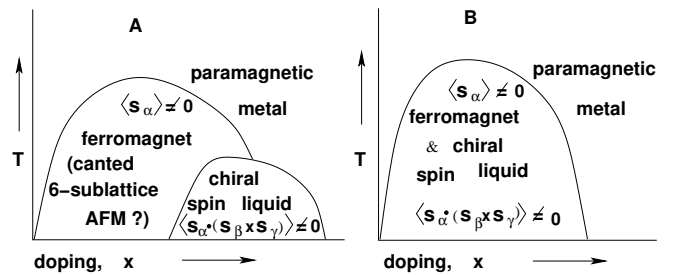


FIG. 2. Two Possible Schematic Phase diagrams in the x - T plane. The experimentally observed ‘ferromagnetic’ phase is suggested to be a canted 6-sublattice antiferromagnetic or a chiral spin liquid phase

In a double exchange [21] process, an added electron prefers higher total spins such as 2 or 1 between neighboring B spin-1 pairs, in order to satisfy Hund's rule during delocalization; *singlet pairs are bottle necks for doped carrier delocalization*. In the VBS phase such singlet amplitudes among neighboring spin pairs within an octahedron are relatively low: total spin values 2, 1 and 0 of a pair occur with probabilities $\sim \frac{5}{9}, \frac{3}{9}$ and $\frac{1}{9}$; on the other hand the singlet amplitude is larger ~ 1 at an octahedral bridge pair. Carrier delocalization thus will selectively project out large local singlets from the bridge pairs; i.e., it effectively adds a local term, a singlet projector, $xt_{\pi 2}(\mathbf{S}_{i\alpha} + \mathbf{S}_{j\beta})^2$, to the singlet dominated octahedral bridge pair. Thus J_1 and J_2 of our spin Hamiltonian (equation 2) get modified in a *state dependent fashion* to effective $\tilde{J}_2(x) \approx J_2 - xt_{\pi 2}$ and $\tilde{J}_1(x) \approx J_1$.

The above results in a linear decrease in the ratio with doping x : $\frac{\tilde{J}_2(x)}{\tilde{J}_1(x)} \sim \frac{J_2}{J_1} - x \frac{t_{\pi 2}}{J_1}$. Thus doping may allow us to enter (in figure 1) the 6-sublattice AFM phase (with a small canting induced ferromagnetism, to be discussed below) or a quantum melted version with long range chiral order. The scale of maximum T_c in our picture is roughly the maximum scale of T_c of the insulating part of the phase diagram, determined by J_1 J_2 : $k_B T_c \approx J_1$, J_2 , which can be easily as large as 900 K.

Once we establish a well developed short range or long range AFM order canting is easily obtained in the double exchange mechanism, as explained by de Gennes in 1960 in the context of doped manganites. This is explained by minimizing the sum of the exchange energy of an octahedral bridge pair spins, for example, and the Anderson-Hasegawa double exchange term [21]:

$$E \approx J_2 \cos \theta - t_{\pi 2} x \cos \frac{\theta}{2} \quad (4)$$

Here θ is the angle between the two spins. The energy minimum occurs at $\cos \frac{\theta}{2} = \frac{t_{\pi 2} x}{J_2}$, i.e., $\theta \approx 180^\circ - \frac{t_{\pi 2} x}{J_2}$, rather than at $\theta = 180^\circ$. This leads to a small moment of $\approx 0.9 \mu_B$ per formula unit, close to what is seen experimentally.

The preexisting planar chirality (vorticity) in our 6-sublattice AFM order, elaborated earlier, gives us a novel possibility of a finite non-planar chirality order [22] $\langle \mathbf{S}_{i\alpha} \cdot (\mathbf{S}_{i\beta} \times \mathbf{S}_{i\gamma}) \rangle \neq 0$, through quantum fluctuations arising from dopant carrier delocalization. How canting, a net magnetic moment and a non-planar chirality arise through quantum fluctuations is nicely illustrated in the following example. Consider three spin-half moments coupled antiferromagnetically: $H = J(\mathbf{S}_1 \cdot \mathbf{S}_2 + \mathbf{S}_2 \cdot \mathbf{S}_3 + \mathbf{S}_3 \cdot \mathbf{S}_1)$ has a 120° classical planar ground state ($S_z = 0$) with a two fold planar chirality degeneracy. However, the exact ground states have non-planar chirality $\langle \mathbf{S}_1 \cdot (\mathbf{S}_2 \times \mathbf{S}_3) \rangle_G = \pm 2\sqrt{3}$ and a net spin $= \frac{1}{2}$ moment, both arising from quantum fluctuation induced canting. One should not also rule out the possibility of nematic

order such as $\langle \mathbf{S}_\alpha \times \mathbf{S}_\beta \rangle_G \neq 0$ in view of the complexity in our system.

Thus canting, weak moment ferromagnetism and development of non-zero chiral order parameter $\langle \mathbf{S}_{i\alpha} \cdot (\mathbf{S}_{i\beta} \times \mathbf{S}_{i\gamma}) \rangle \neq 0$ are all tied together. As the energy scales and the origin of the chirality stiffness and the 6-sublattice AFM stiffness are different the carrier delocalization can also quantum melt the long range AFM order but leave the chirality order intact. In this case we will have a chiral spin liquid with a weak ferromagnetic moment. Figure 2 gives two schematic phase diagrams in the $x - T$ plane.

Important questions as to why ferromagnetism occur in a narrow range of doping x , the complex transport, and sharpening our various estimates and heuristic arguments by many body methods remains to be done.

I thank P.W. Anderson for an encouraging discussion.

-
- [1] D.P. Young et al., Nature **397** 412 (99)
 - [2] H. Ott et al., Physica **B281-282** 423 (00)
 - [3] P. Vonlanthen et al., Phys. Rev. **B62** 10076 (00)
 - [4] R.R. Urbano et al., cond-mat/0106550
 - [5] J.L. Gavilano, cond-mat/0011352
 - [6] T. Terashima et al., J. Phys. Soc. Jap., **69** 2423 (00); T. Morikawa, T. Nishioka and N.K. Sato, *ibid*, **70** 341 (01); S. Kunii, *ibid* **69** 3789 (00)
 - [7] J.D. Denlinger et al., cond-mat/0107426; J.D. Denlinger et al., cond-mat/0107429
 - [8] D. Ceperley, Nature, **397** 386 (99)
 - [9] B.A. Volkov et al., Sov. Phys. JETP, **41** 952 (76); *ibid.*, **43** 589 (76)
 - [10] M.E. Zhitomirsky, T.M. Rice and V.I. Anisimov, Nature, **402** 251 (99); M.E. Zhitomirsky and T.M. Rice, Phys. Rev. **B62** 1492 (00); T. A. Gloré, M.E. Zhitomirsky and T.M. Rice, Euro. Phys. J., **B21** 491 (01); S. Murakami et al., cond-mat/0107215
 - [11] L. Balents and C.M. Varma, Phys. Rev. Lett., **84** 1264 (00); M.Y. Veillette and L. Balents, cond-mat/0105245
 - [12] V. Barzykin and L.P. Gor'kov, Phys. Rev. Lett., **84** 2207 (00)
 - [13] T. Ichinomiya, cond-mat/0009290
 - [14] R. Monnier and B. Delley, cond-mat/0105210
 - [15] H.C. Longuet-Higgins and M de V Roberts, Proc. Roy. Soc. **224** 336 (54)
 - [16] A. Hasegawa and A. Yanase, J. Phys. **C12** 5431 (79)
 - [17] S. Massidda et al., Z. Phys. **B102** 83 (97); C.O. Rodriguez, R. Weht and W.E. Pickett, cond-mat/0003201
 - [18] H.J. Tromp et al., Phys. Rev. Lett., **87** 16401 (01)
 - [19] I. Affleck et al., Phys. Rev. Lett., **59** 799 (87)
 - [20] G. Baskaran (unpublished)
 - [21] P.W. Anderson and H. Hasegawa, Phys. Rev. **100** 675 (55); P.G. de Gennes, Phys. Rev., **118** 141 (60)
 - [22] V. Kalmayer and R.B. Laughlin, Phys. Rev. Lett., **59** 2095 (87)